Available online at www.sciencedirect.com
ScienceDirect
Journal of Organometallic Chemistry 692 (2007) 2911–2923
Journal of Organometallic Chemistry
www.elsevier.com/locate/jorganchem

A novel heterobidentate chiral phosphine and its coordination chemistry in transition metal clusters

Marina M. Tomashevskaya [a], Sergey P. Tunik [a,*], Ivan S. Podkorytov [b], Brian T. Heaton [c,*], Jonathan A. Iggo [c], Matti Haukka [d], Tapani A. Pakkanen [d], Päivi L. Pirilä [e], Jouni Pursiainen [f]

[a] *Department of Chemistry, St. Petersburg State University, Universitetskii pr., 26, St. Petersburg 198504, Russia*
[b] *S.V. Lebedev Central Synthetic Rubber Research Institute, Gapsalskaya 1, St. Petersburg 198035, Russia*
[c] *Department of Chemistry, University of Liverpool, P.O. Box 147, Liverpool L69 7ZD, UK*
[d] *Department of Chemistry, University of Joensuu, P.O. Box 111, FIN-80101 Joensuu, Finland*
[e] *Biocenter Oulu and Department of Biochemistry, P.O. Box 3000, FIN-90014 University of Oulu, Finland*
[f] *Department of Chemistry, P.O. Box 3000, FIN-90014 University of Oulu, Finland*

Received 7 November 2006; received in revised form 23 February 2007; accepted 2 March 2007
Available online 14 March 2007

Abstract

The optically active ligand *R*,*R*-PHAZAN (1,3-*bis*[(1*R*)-1-Phenylethyl]-2-(2-thienyl)-1,3,2-diazaphospholane) has been prepared and the products resulting from the reactions with $Rh_6(CO)_{15}NCMe$, $H_3RhOs_3(CO)_{12}$, and $H_4Ru_4(CO)_{12}$ have been investigated by X-ray crystallography and a variety of multinuclear NMR methods. X-ray studies show that PHAZAN can behave as a bidentate ligand in $Rh_6(CO)_{14}(\mu_2,\kappa^2$-*R*,*R*-PHAZAN) (with coordination through P and S) or a monodentate ligand (through P coordination) in $H_4Ru_4(CO)_{11}(\kappa^1$-*R*,*R*-PHAZAN) and NMR studies show that these structures are retained in solution. In $Rh_6(CO)_{14}(\mu_2,\kappa^2$-*R*,*R*-PHAZAN), edge-bridging coordination of PHAZAN results in the formation of an additional two novel chiral centres and these are observed in solution. Reaction of PHAZAN with $H_3RhOs_3(CO)_{12}$ results in cleavage of the thienyl group and formation of the phosphido cluster, $H_2RhOs_3(CO)_{11}(\mu_2$-PNN), (PNN = 1,3-*bis*-(1-phenylethyl)-[1,3,2]diazaphospholidine-2-yl). A variety of NMR measurements show that the hydride site-occupancies in the solid state are retained in solution and there is evidence for interaction of an *ortho*-phenyl hydrogen and a hydride through ''dihydrogen'' bonding.

Keywords: Cluster compounds; Phosphines; X-ray diffraction; NMR spectroscopy; Asymmetry; Nuclear Overhauser effect

1. Introduction

In the fast-developing area of asymmetric catalysis, tuning of the reactivity of the catalysts and the chiral induction in a particular reaction are of primary importance. One of the main ways to reach this goal relys upon the directed modification of steric and electronic properties of the chiral ligands determining stereoinduction of the catalysts. This stimulates growing interest in the synthesis of novel chiral ligands, which is a booming field of academic research and fine-chemicals business. In this area, phosphines are extremely versatile ligands; they may include a broad range of chiral auxiliaries incorporated into the structure of the phosphines with a particular rigid organic fragment. Among these chiral fragments 1-phenylethylamine is an easily available and relatively inexpensive starting synthon, which allows a flexible design of asymmetric auxiliaries in the ligands of various nature. One of the simplest and

* Corresponding authors. Tel.: +7 812 4284028; fax: +7 812 4286939 (S.P. Tunik).
E-mail address: stunik@chem.spbu.ru (S.P. Tunik).

0022-328X/$ - see front matter © 2007 Elsevier B.V. All rights reserved.
doi:10.1016/j.jorganchem.2007.03.008

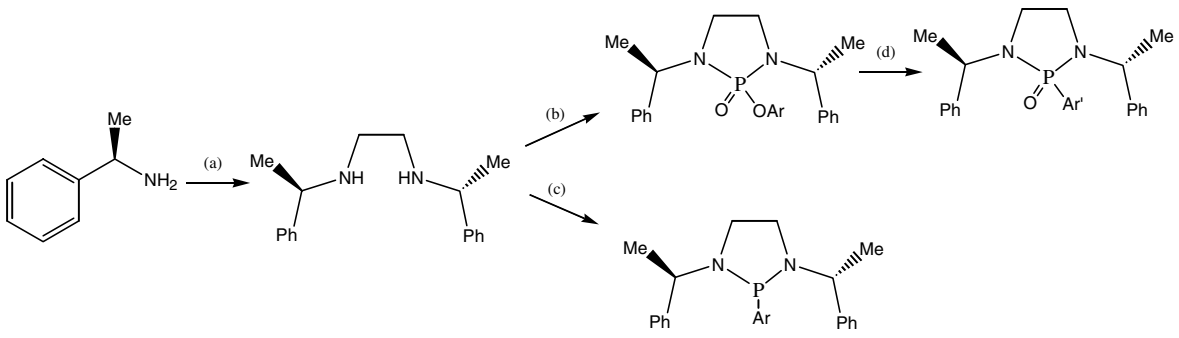

Scheme 1. (a) $BrCH_2CH_2Br$, Et_3N, 115 °C; (b) $ArOP(O)Cl_2$, Et_3N/CH_2Cl_2, rt; (c) $ArPCl_2$, Et_3N/THF, −50 °C; (d) *n*-BuLi/THF, −78 °C.

effective ways to introduce this chiral fragment into the structure of a phosphorus containing ligand is the condensation of dichlorophosphine or dichlorophosphine oxide with the diamine derived from 1-phenylethylamine, see Scheme 1.

This synthetic approach has been applied to obtain the corresponding chiral phosphines [1,2] and phosphine oxides [3,4], which were further used in asymmetric catalysis [1,4–8], as chiral inductors in stoichiometric reactions [3,9–11] and as probing reagents for establishing the enantiomeric excess by means of ^{31}P NMR spectroscopy [12–15].

It is quite surprising that despite the wide use of these ligands in catalysis there have been no reports on the studies of their coordination chemistry neither in mono- nor in poly-nuclear metal complexes. It is worth noting that asymmetric induction of these ligands can be substantially improved by functionalization of the third substituent at the phosphorus atom [4]. These structural modifications may provide an additional interaction of the ligands with catalytic substrates or allow their multidentate coordination thus supporting the conformational rigidity of the catalyst chiral pocket. Understanding of the nature of these effects, as well as the directed tuning of the catalytic enantioselectivity requires an investigation of the coordination chemistry of the ligand, the structure and properties of the corresponding complexes. In the present paper, we report the synthesis of a related bidentate phosphine (**2**) containing an additional thienyl coordinating function and describe the study of the coordination chemistry of (**2**) in tetra- and hexa-nuclear carbonyl clusters.

2. Experimental

2.1. General comments

Reagent grade (*R*)-(+)-1-phenylethylamine (Acros), 1,2-dibromoethane and Et_3N were used without further purification. Dichloro(thiophene-2-yl)phosphine [16], $Rh_6(CO)_{15}(NCMe)$ [17], $H_4Ru_4(CO)_{12}$ [18], and $H_3Os_3Rh(CO)_{12}$ [19] were synthesized according to published procedures. All solvents were dried over appropriate drying agents and distilled prior to use. The reaction of the cluster compounds with the chiral phosphine was carried out under an argon atmosphere using standard Schlenk techniques. Products were separated in air by column chromatography on silica (5-40 mesh) (Lenchrom Ltd., St. Petersburg). Elemental analysis was carried out in the analytical laboratory of the University of Joensuu. EI and ESI mass spectra were recorded on MX-1321 and Bruker BioAPEX II 47e instruments, respectively. Fast atom bombardment (FAB+) mass spectra were obtained on a Trio 2000 instrument. The IR spectra were measured using a Specord M80 spectrophotometer. CD spectra were recorded on a Jasco J-715 spectropolarimeter.

2.2. NMR measurements

^1H, ^{13}C and ^{31}D NMR spectra were recorded on a Bruker DPX 300 instrument. HMQC spectra were recorded on a Bruker AMX2 200 or Avance2 400 spectrometer as previously described [20].

2.3. N,N′-bis(1-(R)-1-phenylethylamine)-1,2-ethylenediamine (1)

A solution of (*R*)-(+)-1-phenylethylamine (5.16 g, 43 mmol), 1,2-dibromethane (1.88 g, 10 mmol) and Et_3N (2.02 g, 20 mmol) in acetonitrile was placed into an ace pressure tube and heated in an oil bath (110 °C) for 15 h. By this time, the reaction mixture darkened and $Et_3N \cdot HBr$ was precipitated. The solution was then filtered and concentrated in vacuo to give a viscous yellow oil, which was diluted with CH_2Cl_2 (15 cm^3) and washed (2×10 cm^3) with KOH 5% aqueous solution saturated with NaCl. The organic layer was dried over sodium sulfate, concentrated and distilled under reduced pressure. The excess (*R*)-(+)-1-phenylethylamine (3.57 g) was distilled off at 78–80 °C (18 mm Hg) and the product (**1**) (1.93 g, 73%) was obtained as the second fraction of the distillation, bp 205 °C/4 mm Hg. The compound was identified by comparison of its spectroscopic characteristics with the literature data [21].

2.4. 1,3-bis[(1R)-1-Phenylethyl]- 2-(2-thienyl)-1,3,2-diazaphospholane-R,R-PHAZAN) (2)

Dicloro(thiophene-2-yl)phosphine (0.28 g, 1.5 mmol) was added dropwise at −50 °C under an argon atmosphere to a solution of *N*,*N*′-*bis*(1-(*R*)-1-phenylethylamine)-1,2-ethylenediamine (**1**) (0.40 g, 1.5 mmol) and Et_3N (0.31 g, 1.5 mol) in THF (8 cm^3). The resulting mixture was allowed to warm up to room temperature and stirred for another 0.5 h. The precipitate of $Et_3N \cdot HCl$ was filtered off and the filtrate concentrated in vacuo to give a viscous pale yellow oil. It was dissolved in THF (1 cm^3) and the desired product was extracted with hexane (4 × 5 cm^3). The solvent was removed and the residue (colourless oil) was dried in vacuo for 5 h to give 0.43 g of (**2**). The product was left for a month at −20 °C under an argon atmosphere to give a white amorphous solid. Yield 80%, mp 42 °C. ^{1}H NMR (300 MHz, $CDCl_3$, 25 °C): $\delta = 7.60$ (d, $J = 4.4$ Hz, 1H, thienyl), 7.12–7.48 (m, 12H, ArH), 4.10 (pseudo-quintet, $J = 6.6$ Hz, 1H, CH), 3.72 (pseudo-quintet, $J = 6.6$ Hz, 1H, CH), 2.72–3.15 (m, 4H, CH_2), 1.65 (d, $^4J_{H-P} = 6.6$ Hz, 3H, CH_3), 1.55 (d, $^4J_{H-P} = 5.5$ Hz, 3H, CH_3), ^{13}C NMR (75 MHz, $CDCl_3$, 25 °C): phenyl and thienyl signals: $\delta = 145.81$, 145.75, 145.56, 145.46, 132.98, 132.60, 130.52, 128.94, 128.77, 128.67, 128.10, 128.04, 127.67, 127.62, 127.54, 127.39, 127.35, 127.22, 60.15 (d, $^2J_{C-P} = 87.2$ Hz, CH), 58.94 (d, $^2J_{C-P} = 47.6$ Hz, CH), 50.03 (d, $^2J_{C-P} = 31.7$ Hz, CH_2), 49.83 (d, $^2J_{C-P} = 35.7$ Hz, CH_2), 24.86 (d, $^3J_{C-P} = 59.5$ Hz, CH_3), 23.58 (d, $^3J_{C-P} = 71.4$ Hz, CH_3). ^{31}P NMR (121 MHz, $CDCl_3$, 25 °C): $\delta = 79.94$ (s). EI MS (*m*/*z*): 380 (M^+) (calc 380). Anal. Calc. for $C_{22}H_{25}N_2PS$: C, 69.45; H, 6.62; N 7.36. Found: C, 69.39; H, 6.82; N 7.26%.

2.5. $Rh_6(CO)_{14}(\mu_2$-R,R-PHAZAN) (3)

A mixture of $Rh_6(CO)_{15}NCMe$ (80 mg, 0.074 mmol) and *R*,*R*-PHAZAN (31 mg, 0.081 mmol) in degassed $CHCl_3$ (50 cm^3) was stirred for 1.5 h at 40 °C. By this time, a TLC spot test (eluent CH_2Cl_2–hexane (1/2 v/v)) showed the presence of the major product (red-brown band) and a minor one (brown band). The reaction mixture was concentrated in vacuo to ca. 1.5 cm^3, diluted with hexane (3 cm^3) and transferred onto a chromatographic column (2.5 × 13 cm). Separation with CH_2Cl_2–hexane (1/2 v/v) mixture gave the following bands in the order of elution: trace amount of $Rh_6(CO)_{16}$; $Rh_6(CO)_{15}(\kappa^1$-(R/R)-PHAZAN) (5 mg, 5%) and $Rh_6(CO)_{14}(\mu,\kappa^2$-*R*,*R*-PHAZAN) (**3**, 65 mg, 64%).

IR ($CHCl_3$, cm^{-1}), *ν*(CO) 2090 m, 2060 vs, 2032 m, 2005 w, 1782 w, br. ^{1}H NMR (300 MHz, $CDCl_3$, 25 °C, * major diastereomer, **minor diastereomer): $\delta =$ **7.66 (t, $J =$ 4.4 Hz, 1H, thienyl), *7.63 (t, $J = 4.4$ Hz, 1H, thienyl), 7.29–7.58 (m, 10H, Ph), *7.05 (t, $J = 4.4$ Hz, 1H, thienyl), **7.01 (t, $J = 4.4$ Hz, 1H, thienyl), 6.13 (dd, $J = 4.4$, 2.2 Hz, 1H, thienyl), **5.48–5.60 (m, 2H, CH), *5.21–5.38 (m, 2H, CH), 2.91–3.33 (m, 4H, CH_2), **1.74 (d, $J = 6.6$ Hz, 3H, CH_3), **1.61 (d, $J = 6.6$ Hz, 3H, CH_3), *1.59 (d, $J = 9.0$ Hz, 3H, CH_3), *1.42 (d, $J = 9.0$ Hz, 3H, CH_3). ^{31}P NMR (121 MHz, $CDCl_3$, 25 °C, * major diastereomer, **minor diastereomer): $\delta =$ **89.23 (d, $J_{Rh-P} =$ 173 Hz), *88.84 (d, $J_{Rh-P} = 173$ Hz). MS-FAB (*m*/*z*): 1390 (M^+) (calc 1390), [$M^+ - n$CO], $n = 1$–14. Anal. Calc. for $C_{36}H_{25}N_2O_{14}PSRh_6$: C, 31.11; H, 1.81; N 2.02. Found: C, 31.23; H, 1.86; N 2.08%. Single crystals of **3** suitable for X-ray analysis were obtained by slow evaporation of the hexane solution at −20 °C.

2.6. $H_2RhOs_3(CO)_{11}$(PNN) (4)

A solution of $H_3RhOs_3(CO)_{12}$ (25 mg, 0.025 mmol) and *R*,*R*-PHAZAN) (11 mg, 0.028 mmol) in degassed $CHCl_3$-(25 cm^3) was stirred at room temperature for 30 min under an argon atmosphere. By this time, the colour of the mixture turned orange and a TLC spot test (eluent CH_2Cl_2–hexane (2/5 v/v)) showed the presence of one major product and some starting cluster. The reaction mixture became bright-yellow after stirring at 40 °C for 30 min. A TLC spot test showed complete consumption of the starting cluster and formation of a new product. The solvent was then evaporated under reduced pressure, the resulting mixture was diluted with CH_2Cl_2 (1.5 cm^3) and hexane (3 cm^3) and transferred onto a chromatographic column (2 × 10 cm). Careful separation gave the cluster **4** as a major product (23 mg, 72%).

IR ($CHCl_3$, cm^{-1}), *ν*(CO) 2090 m, 2060 s, 2027 vs, 2012 sh, 1990 m, 1980 sh, 1870 w, br. ^{1}H NMR (300 MHz, $CDCl_3$, 25 °C): $\delta = 7.29$–7.53 (m, 10H, Ph), 4.34–4.50 (m, 1H, CH), 4.00–4.15 (m, 1H, CH), 3.47-3.75 (m, 2H, CH_2), 3.23–3.39 (m, 2H, CH_2), 1.69 (d, $J = 6.6$ Hz, 3H, CH_3), 1.67 (d, $J = 6.6$ Hz, 3H, CH_3), −22.63 (d, $J_{H-P} =$ 6.5 Hz, 1H, hydride), −22.74 (d, $J_{H-P} = 6.5$ Hz, 1H, hydride). ^{31}P NMR (121 MHz, $CDCl_3$, 25 °C): $\delta = 259.7$ (s). MS-FAB (*m*/*z*): 1282 (M^+) (calc. 1282), [$M^+ - n$CO], $n = 1$–11. Anal. Calc. for $C_{39}H_{24}N_2O_{11}PRhOs_3$: C, 27.19; H, 1.89; N 2.19. Found: C, 27.13; H, 1.88; N 2.20%.

Single crystals of **4** suitable for X-ray analysis were obtained by slow diffusion of hexane into a CH_2Cl_2solution at −3 °C.

2.7. $H_4Ru_4(CO)_{11}(\kappa^1$-R,R-PHAZAN) (5)

$H_4Ru_4(CO)_{12}$ (60 mg, 0.080 mmol) and *R*,*R*-PHAZAN) (34 mg, 0.088 mmol) were dissolved in degassed $CHCl_3$ (35 cm^3) and a solution of $Me_3NO.2H_2O$ (9 mg, 0.088 mmol) in 10 cm^3 $CHCl_3$ was added dropwise with vigorous stirring. The reaction mixture was stirred at 50 °C until a TLC spot test (eluent CH_2Cl_2–hexane (1/3 v/v)) showed complete consumption of the starting cluster into the major product (orange band). The solvent was then removed in vacuo, the residue dissolved in CH_2Cl_2 (1.3 cm^3) and diluted with hexane (3 cm^3) leaving some amorphous crystalline material, which was filtered off. The solution obtained was purified by column chromatography (2.5 ×

12 cm) using CH_2Cl_2–hexane (1/3 v/v) mixture as eluent. The following products were isolated in the order of elution: trace amount of $H_4Ru_4(CO)_{12}$ and a main orange band of (**5**) (42 mg, 48%).

IR ($CHCl_3$, cm^{-1}), ν(CO) 2092 m, 2084 m, 2058 s, 2024 s. ^1H NMR (300 MHz, $CDCl_3$, 25 °C): $\delta = 7.72$ (t, $J = 3.3$ Hz, 1H, thienyl), 7.05–7.62 (m, 10H, Ph), 6.82 (d, $J = 7.7$ Hz, 1H, thienyl), 4.62–4.75 (m, 1H, CH), 4.42–4.54 (m, 1H, CH), 3.16–3.33 (m, 1H, CH_2), 2.75–3.12 (m, 3H, CH_2), 1.60 (d, $J = 6.6$ Hz, 3H, CH_3), 1.58 (d, $J = 6.6$ Hz, 3H, CH_3), −17.29 (br. s, 4H, hydrides). Hydride signals at −50 °C: −17.21 (d, $J_{H-P} = 4.9$ Hz, 2H), −17.46 (d, $J_{H-P} = 13.3$ Hz, 1H), −17.59 (d, $J_{H-P} = 9.5$ Hz, 1H). ^{31}P NMR (121 MHz, $CDCl_3$, 25 °C): $\delta = 108.6$ (s). MS-FAB (m/z): 1098 (M^+) (calc 1098), [$M^+ - nCO$], $n = 1$–11. Anal. Calc. for $C_{33}H_{29}N_2O_{11}PSRu_4$: C, 36.13; H, 2.66; N 2.55. Found: C, 36.28; H, 2.83; N, 2.32%. Single crystals of **5** suitable for X-ray analysis were obtained by slow diffusion of hexane into a CH_2Cl_2 solution in the presence of a few drops of methanol at −20 °C.

3. X-ray crystal structure determinations

The crystals were immersed in cryo-oil, mounted in a Nylon loop and measured at a temperature of 120 K. The X-ray diffraction data was collected by means of a Nonius Kappa CCD diffractometer using Mo Kα radiation ($\lambda = 0.71073$ Å). The Denzo-Scalepack [22] program package was used for cell refinements and data reductions. All of the structures were solved by direct methods using the SIR97, SIR2004, or SHELXS-97 [23–25] with the WINGX [26] graphical user interface. An empirical absorption correction was applied to all of the data (XPREP in SHELXTL v.6.14-1) [27]. Structural refinements were carried out using SHELXL-97 [28]. The thiophene ring in **5** was disordered having two orientations. The S1 and C33 atoms were refined over two positions with equal coordinates and occupancies of 0.84 and 0.16. The idealized positions of the hydride hydrogens in **4** and **5** were estimated with XHYDEX [29] program. All other hydrogens were positioned geometrically and allowed to ride on their parent atoms. The crystallographic details are summarized in Table 1 and the selected bond lengths and angles in Table 2.

4. Results and discussion

1,3-bis[(1*R*)-1-Phenylethyl]-2-(2-thienyl)-1,3,2-diazaphospholane *R,R*-PHAZAN) was synthesized according to Scheme 2.

To optimize the yield of *N,N′-bis*(1-(*R*)-1-Phenylethylamine)-1,2-ethylenediamine, the synthesis was carried out in an ace pressure tube under high temperature and pressure. The reaction of the diamine with dicloro(thiophene-2-yl)phosphine gave the phosphine (**2**) as a white amorphous solid in high yield. The structure of (**2**) was determined using ^1H, ^{13}C and ^{31}P NMR spectroscopy. As expected, the diamine (**1**) and the phosphine (**2**) display nearly identical Cotton responses in their CD spectra below 280 nm (Fig. S1) which is indicative of the same source of asymmetry in both compounds. The coordination behaviour of (**2**) relies upon the presence of the phosphorus and thienyl coordinating functions, which in principle allow bridging or chelating coordination of this ligand in polynuclear transition metal complexes.

4.1. $Rh_6(CO)_{14}(\mu_2$-*R,R*-PHAZAN) (**3**)

Reaction of the labile cluster, $Rh_6(CO)_{15}NCMe$, with the PHAZAN ligand, accompanied by warming the reac-

Table 1
Crystal data and structure refinement for **3**, **4** and **5**

	$Rh_6(CO)_{14}(\mu_2$-κ^2-*R,R*-PHAZAN) (**3**)	$H_2RhOs_3(CO)_{11}(\mu_2$-PNN) (**4**)	$H_4Ru_4(CO)_{11}(\kappa^1$-*R,R*-PHAZAN) (**5**)
Empirical formula	$C_{36}H_{25}N_2O_{14}PRh_6S$	$C_{29}H_{24}N_2O_{11}Os_3PRh$	$C_{33}H_{29}N_2O_{11}PRu_4S$
Molecular weight	1390.07	1280.98	1096.89
Crystal system	Monoclinic	Monoclinic	Orthorhombic
Space group	$P2_1$	$P2_1$	$P2_1\ 2_1\ 2_1$
a (Å)	9.42510(10)	18.1671(5)	9.14450(10)
b (Å)	17.8492(3)	8.2765(2)	17.4658(2)
c (Å)	12.82930(10)	23.6046(3)	24.1155(3)
α (°)	90	90°	90
β (°)	104.9470(10)	108.5130(10)	90
γ (°)	90	90	90
V (Å^3)	2085.25(4)	3365.52(13)	3851.63(8)
T (K)	120(2)	120(2)	120(2)
Z	2	4	4
D_{calc} (g cm^{-3})	2.214	2.528	1.892
μ (mm^{-1})	2.475	11.879	1.692
Number of reflections collected	31989	56755	54062
Number of unique reflections	9459	15254	8811
R_{int}	0.0415	0.0730	0.0623
R^a	0.0243	0.0499	0.0271
$wR2^a$	0.0483	0.1187	0.0474

[a] $I > 2\sigma$.

Table 2
Selected bond lengths in $Rh_6(CO)_{14}(\mu_2,\kappa^2$-*R*,*R*-PHAZAN) (**3**), $H_2RhOs_3(CO)_{11}(\mu_2$-PNN) (**4**) and $H_4Ru_4(CO)_{11}(\kappa^1$-*R*,*R*-PHAZAN) (**5**)

(**3**)		(**4**)		(**5**)	
Rh(1)–Rh(2)	2.7647(4)	Os(1)–Rh(1)	2.7325(14)	Ru(1)–Ru(4)	2.7972 (3)
Rh(1)–Rh(6)	2.7776(4)	Os(1)–Os(2)	2.8762(8)	Ru(1)–Ru(2)	2.9699 (3)
Rh(1)–Rh(5)	2.7876(4)	Os(1)–Os(3)	2.9739(8)	Ru(1)–Ru(3)	2.9760 (4)
Rh(1)–Rh(4)	2.8016(4)	Os(2)–Rh(1)	2.7680(14)	Ru(2)–Ru(3)	2.7912 (3)
Rh(2)–Rh(3)	2.7097(4)	Os(2)–Os(3)	2.9871(8)	Ru(2)–Ru(4)	2.9729 (4)
Rh(2)–Rh(5)	2.7152(4)	Os(3)–Rh(1)	2.7328(14)	Ru(3)–Ru(4)	2.9672 (4)
Rh(2)–Rh(6)	2.7376(4)			Average[a]	2.901 (88)
Rh(3)–Rh(6)	2.7613(4)	Os(1)–C(1)	1.882(16)		
Rh(3)–Rh(4)	2.7638(4)	Os(1)–C(2)	1.899(18)	Ru(1)–C(2)	1.880(4)
Rh(3)–Rh(5)	2.7949(4)	Os(2)–C(5)	1.861(17)	Ru(1)–C(1)	1.882(4)
Rh(4)–Rh(5)	2.7287(4)	Os(2)–C(4)	1.891(18)	Ru(2)–C(3)	1.900(4)
Rh(4)–Rh(6)	2.7634(4)	Os(3)–C(7)	1.888(17)	Ru(2)–C(5)	1.910(4)
Average[a]	2.759(29)	Os(3)–C(8)	1.925(16)	Ru(2)–C(4)	1.933(4)
		Os(3)–C(9)	1.926(19)	Ru(3)–C(6)	1.894(4)
Average[a]. Rh–C(O)^{term}	**1.900(10)**	Rh(1)–C(10)	1.873(15)	Ru(3)–C(8)	1.905(4)
		Rh(1)–C(11)	1.892(16)	Ru(3)–C(7)	1.922(4)
Rh(1)–C(2)	2.184(4)	Os(1)–C(3)	2.082(16)	Ru(4)–C(10)	1.892(4)
Rh(2)–C(2)	2.140(4)	Rh(1)–C(3)	2.200(17)	Ru(4)–C(9)	1.897(4)
Rh(5)–C(2)	2.238(4)	Os(2)–C(6)	2.035(15)	Ru(4)–C(11)	1.947(3)
Rh(1)–C(9)	2.153(4)	Rh(1)–C(6)	2.283(14)	Average[a]	1.905(20)
Rh(4)–C(9)	2.211(4)				
Rh(6)–C(9)	2.185(4)	Os(1)–P(1)	2.363(4)		
Rh(2)–C(7)	2.112(4)	Os(2)–P(1)	2.353(4)		
Rh(3)–C(7)	2.244(4)				
Rh(6)–C(7)	2.222(4)				
Rh(3)–C(6)	2.200(4)				
Rh(4)–C(6)	2.217(4)				
Rh(5)–C(6)	2.159(4)				
Average[a]	2.189(39)				
Rh(1)–P(1)	2.3017(9)				
Rh(2)–S(1)	2.3830(9)				
S(1)–C(15)	1.745(4)				
P(1)–C(15)	1.821(4)				

[a] Values of variance $S = [(x_i - \bar{x})^2/(n-1)]^{1/2}$ for the averages are given in parentheses.

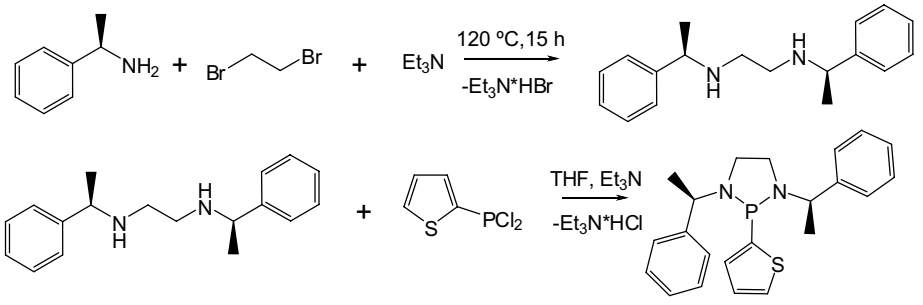

Scheme 2.

tion mixture, readily affords the cluster (**3**) with edge-bridging coordination of the phosphine through phosphorus and thienyl sulfur. The solid state structure of (**3**) was established using X-ray crystallography. An ORTEP view of (**3**) is shown in Fig. 1 with selected structural parameters in Table 2. The ligand occupies two terminal sites on adjacent rhodium atoms to form a five-membered dimetallacycle, which is a typical structural motif for the coordination of thienylphosphines on the Rh_6-framework [30]. The substitution does not change the cluster electron count which corresponds to a closed octahedral structure of the rhodium framework in (**3**). Bond lengths and angles in (**3**) (see Table 2) are not significantly distorted when compared to the closely analogous clusters, $Rh_6(CO)_{14}(\mu,\kappa^2$-$Ph_2PThienyl)$ and $Rh_6(CO)_{14}(\mu,\kappa^2$-$PhPThienyl_2)$ [30]; this is indicative of an essentially non-strained coordination of the bulky PHAZAN ligand. The solid state conformations of the chiral auxiliaries in coordinated PHAZAN allows minimization of the ligand nonbonding interactions with adjacent CO's. The presence of a few short contacts

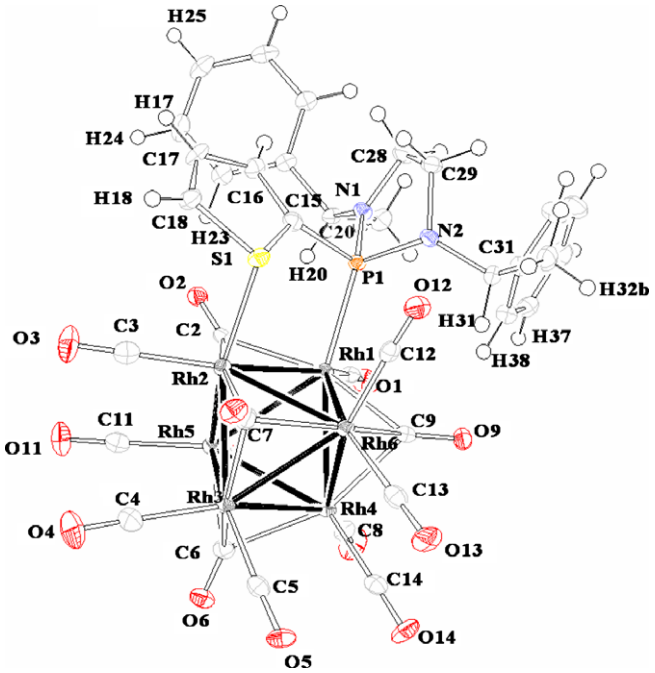

Fig. 1. ORTEP view of $Rh_6(CO)_{14}(\mu_2,\kappa^2\text{-}R,R\text{-PHAZAN})$ (**3**).

(H(20)–O(2) 2.898 Å, H(23)–O(2) 2.545 Å, H(31)–O(9) 2.349 Å, H(38)–O(9) 2.642 Å) does not affect the general motif and particular structural parameters of the carbonyl environment, which is close similar to the other $Rh_6(CO)_{14}(\mu,\kappa^2\text{-PX})$ clusters characterized earlier [30,31].

Edge-bridging coordination of PHAZAN results in the formation of two novel chiral centers in (**3**). One of them is associated with the coordinated tetrahedral sulfur atom whereas the other is a planar chiral "Rh_3PS" fragment [30]. Crystallographic analysis in $P2_1$ group revealed only one isomeric form of the molecule in the crystal cell of (**3**). Stereochemically, this isomer can be assigned to $RR_{PHAZAN}R_SR_{pl}$ configuration, where subscript "S" and "pl" denote conformations of coordinated sulfur and planar chiral fragments, respectively. However, the ^{31}P and ^1H NMR data (Fig. 2) clearly show duplicate sets of signals, with essentially similar spectroscopic characteristics, that points to the presence of two isomeric forms in the bulk sample. Relative intensities of the corresponding resonances in the major and minor sets are 3/1 irrespective of the sample used in the measurements. Appearance of these isomers is most probably due to the formation of two diastereoisomers, which are shown schematically below.

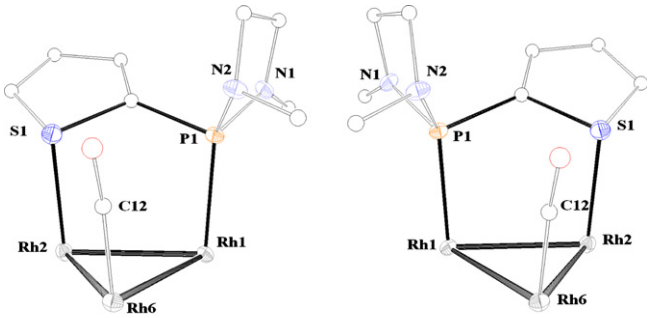

$RR_{PHAZAN}R_SR_{pl}$ $RR_{PHAZAN}S_SS_{pl}$

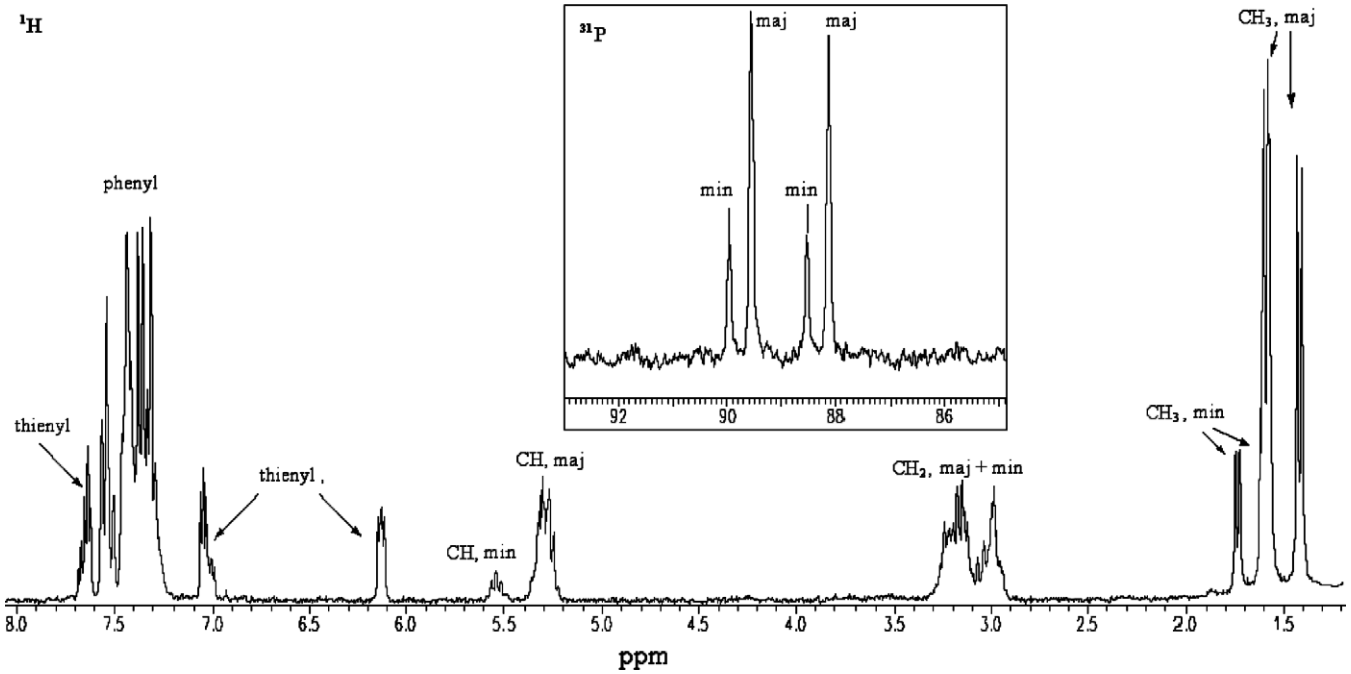

Fig. 2. ^1H and ^{31}P NMR spectra of $Rh_6(CO)_{14}(\mu_2,\kappa^2\text{-}R,R\text{-PHAZAN})$ (**3**), $CDCl_3$, 25 °C. "maj" and "min" denote the signals of major and minor diastereomers of (**3**).

These forms of the molecule differ in stereoconfiguration of the planar chiral "Rh_3PS" fragment (*R* or *S*), which in turn dictates [30] the configuration of the coordinated sulfur to minimize nonbonding interaction of the thienyl ring with the adjacent C(12)O group. The diastereomers are evidently different in the interaction of the ligand chiral auxiliaries with the carbonyl environment of the triangle but this difference is not energetically significant because both configurations are present in solution in comparable amounts. The excess of an isomer with a certain stereoconfiguration of the planar chiral "Rh_3PS" center was also detected by CD measurements, Fig. S2. In addition to the ligand induced Cotton effects below 300 nm, the spectrum of (**3**) displays the absorption bands at 320, and 370 nm that indicates asymmetry of the molecular fragments, which include metal atoms of the cluster skeleton.

Variable temperature ^{31}P measurements (25–70 °C) showed no line broadening and no changes in the relative intensities of the signals that is indicative of conformational rigidity of the isomers in this temperature range. It has to be noted that the rhodium–sulfur bond in (**3**) is not broken by gaseous CO to form a κ^1-coordinated ligand in contrast to structurally analogous Rh_6-alkenylphosphine derivatives studied earlier [32], when the bridging ligand easily breaks the rhodium–alkenyl bond to change the conformation of the alkenyl fragment or is substituted by CO. The carbonyl environment of (**3**) is nonrigid at room temperature and the low temperature limiting spectrum is obtained at −55 °C. The ^{13}C–{^{103}Rh} and ^{31}P–{^{103}Rh} HMQC experiments run at this temperature (Figs. S3 and S4) allow unambiguous assignments of the signals corresponding to the major diastereomer, and these results are summarised in Table 3. The data obtained show that the structure of the carbonyl environment found in the solid state is retained in solution. These spectroscopic data correspond well with the data obtained earlier for the $Rh_6(CO)_{14}(\mu,\kappa^2\text{-}Ph_2PThienyl)$ cluster [31], including the considerable lowfield shift of the signal corresponding to sulfur bound rhodium atom.

4.2. $H_2RhOs_3(CO)_{11}(PNN^*)$ (**4**)

The mixed metal $H_3RhOs_3(CO)_{12}$ cluster readily reacts with *R*,*R*-PHAZAN to give $H_2RhOs_3(CO)_{11}(\mu,\kappa^1\text{-}PNN^*)$ (**4**), containing the phosphide PNN^* ligand coordinated along an Os–Os bond, see Scheme 3.

The phosphide fragment is formed through oxidative cleavage of the P-thienyl bond followed by reductive elimination of thiophene to give (**4**). The solid state structure of (**4**) was established by X-ray crystallography and an ORTEP view of this molecule is shown in Fig. 3; selected structural parameters are given in Table 2. The electron count for (**4**) (60 electrons) fits exactly to a closed tetrahedral structure [33,34] of the cluster framework. The Os–Rh bond lengths fall in a narrow range 2.7325–2.7680 Å, whereas the Os–Os distances differ substantially due to the effects of the ligands coordinated over the osmium triangle. The Os(1)–Os(2) bond (2.8762(8) Å) bridged by the phosphide ligand is considerably shorter compared to the other Os–Os bonds (Os(1)–Os(3) (2.9739(8) Å) and Os(2)–Os(3) (2.9871(8) Å). This observation clearly points to coordination of the hydrides over the latter edges of the cluster skeleton. These effects of the bridging hydrides and phosphides are absolutely typical for osmium clusters [35–45] and can be used to reliably locate the hydride ligands over certain bonds of metal skeleton. This assignment is in agreement with the analysis of the difference Fourier map which allows the site occupancies of the hydrides to be deduced as shown in Fig. 3. This assignment of the site occupancy of the hydrides has been confirmed by NMR measurements, see below. The carbonyl environment of (**4**) consists of 11 CO's, nine of which are terminal and two CO's span Os(1)–Rh(1) and Os(2)–Rh(1) edges. The coordination of the bridging carbonyls along the two Os–Rh edges is strongly asymmetric; the Os–C(O) bond lengths (2.035 and 2.082 Å) are considerably shorter than the Rh–C(O)'s. This is completely in line with the influence of the adjacent phosphide, which increases the electronic density on the osmium atoms to strengthen the basicity of these metal centers and their π-back donation to the corresponding carbonyl ligands. This influence moves the bridging CO's from rhodium towards these osmium atoms.

The solution structure of (**4**) was investigated by a broad range of NMR techniques: ^1H, ^{13}C, ^{31}P, ^{31}P–{^{103}Rh} HMQC, ^{13}C–{^{103}Rh} HMQC and ^1H NOE, see Table 3, Figs. 4, 5, S5, S6 and by CD measurements, Fig. S7. The solid state structure of the isolated "$(\mu\text{-}H)_2Os_3Rh(CO)_9(\mu\text{-}CO)_2(\mu\text{-}P)$" fragment in (**4**), in principle, implies the presence of a symmetry plane through P(1), Os(3) and Rh(1). However, two chiral auxiliaries in the phosphide ligand make the structure of (**4**) asymmetric and give rise to the spectroscopic patterns corresponding to the absence of symmetry elements in the molecule. The coordination sphere of (**4**) is stereochemically rigid at room temperature to give 11 multiplets due to the CO ligands in the carbonyl region of the ^{13}C NMR spectrum. Analysis of the $^{13}C\{^1H\}$ (Table 3) and ^{13}C–{^{103}Rh} HMQC (Fig. S6) spectra together with the ^{13}C–{$^1H_{hydrides}$} selective decoupling experiments (Fig. S5) shows that the structure of the carbonyl environment and mutual disposition of the hydride and carbonyl ligands found in the solid state remain unchanged in solution. The "organic" region of the proton spectrum of (**4**) displays two sets of multiplets (CH_3, CH_2 and CH protons together with unresolved resonance, due to the phenyl rings), Fig. 4, corresponding to inequivalent chiral auxiliaries disposed over and out of the osmium triangle. The two hydrides generate the doublets at −22.74 and −22.63 ppm and the coupling constants, ($^2J(P\text{–}H) = 6.6$ Hz), correspond to a *cis* disposition of the hydrides over adjacent Os–Os bonds [37,41,42,44,45]. It is worth noting that the asymmetry of the {–C(13)HC(14)H_3Ph}-moieties results in a specific orientation the chiral unit with respect to the osmium triangle to minimize nonbonding interaction of the phenyl ring with the nearest

Table 3
The ^{13}C, ^{31}P and ^{103}Rh NMR spectroscopic data for the clusters (**3**) and (**4**)

C(O)[a]	δ, ppm, ^{13}C	J(C–P), Hz	J(C–Rh), Hz		
(**3**)(major isomer) (298 K, $CDCl_3$)					
C(1)O	184.2 dd	11.4	71.6		
C(3)O	181.5 d	–	70.0		
C(4)O	183.7 d	–	65.1		
C(5)O	180.8 d	–	72.3		
C(8)O	180.9 d	–	71.6		
C(14)O	179.7 dd	23.8	69.1		
C(10)O	184.3 d	–	68.2		
C(11)O	183.3 dd	24.7	68.7		
C(12)O	179.6 d	–	69.1		
C(13)O	179.4 d	–	68.2		
μ_3-C(2)O	247.8 s				
μ_3-C(6O	232.5 s				
μ_3-C(7)O	242.2 s				
μ_3-C(9)O	238.4 s				
	^{103}Rh, δ, ppm				
Rh(1)	−308				
Rh (2)	+7				
Rh (3)	−365				
Rh (4)	−383				
Rh (5)	−380				
Rh (6)	−428				
	^{31}P, δ, ppm	J(P–Rh), Hz			
Major isomer	87.7 d	172.3			
Minor isomer	89.8 d	172.3			
C(O)[b]	δ, ppm, ^{13}C	J(C–P), Hz	J(C–Rh), Hz	J(C–H_a), Hz	J(C–H_b), Hz
4(298 K, $CDCl_3$)					
μ_2-C(3)O	211.5 dd	67.6	17.7	–	
μ_2-C(6)O	209.4 dd	65.6	14.5	–	
C(1)O	182.5 d	5.1	–	3.5	
C(4)O	181.3 d	4.3	–	3.5	
C(2)O	168.7 m	5.2	–	–	
C(5)O	167.2 m	–	–	8.9	
C(7)O	172.9 d	2.2			
C(8)O	168.4 s	–	–	3.1	10.8
C(9)O	168.2 s	–	–	10.7	3.0
C(10)O	186.6 dd	–	74.6	5.5	
C(11)O	169.0 d	–	63.0	–	
Hydrides	^1H, δ, ppm	J(H–P)			
H(1)	−22.62	6.6			
H(2)	−22.73	6.6			
	^{31}P, δ, ppm				
P	259.7 s				

[a] Assignment can be reversed for the following resonances: C(4)O/C(5)O, C(12)O/C(13)O.
[b] Assignment can be reversed for the following resonances: C(3)O/C(6)O, C(1)O/C(4)O, C(2)O/C(5)O.

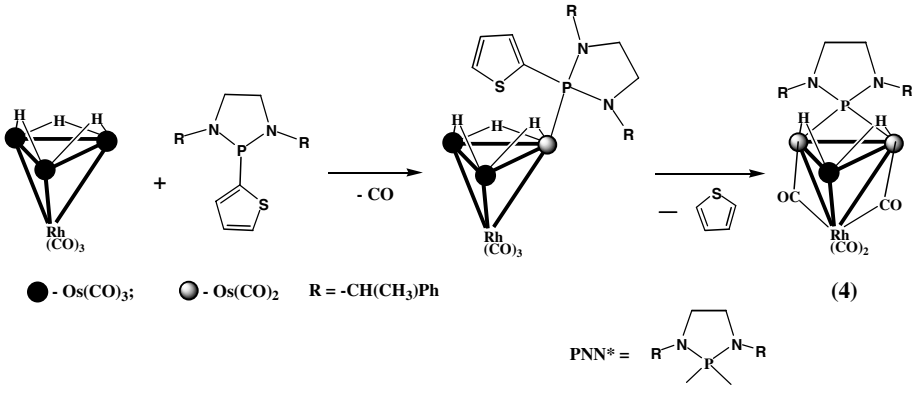

Scheme 3.

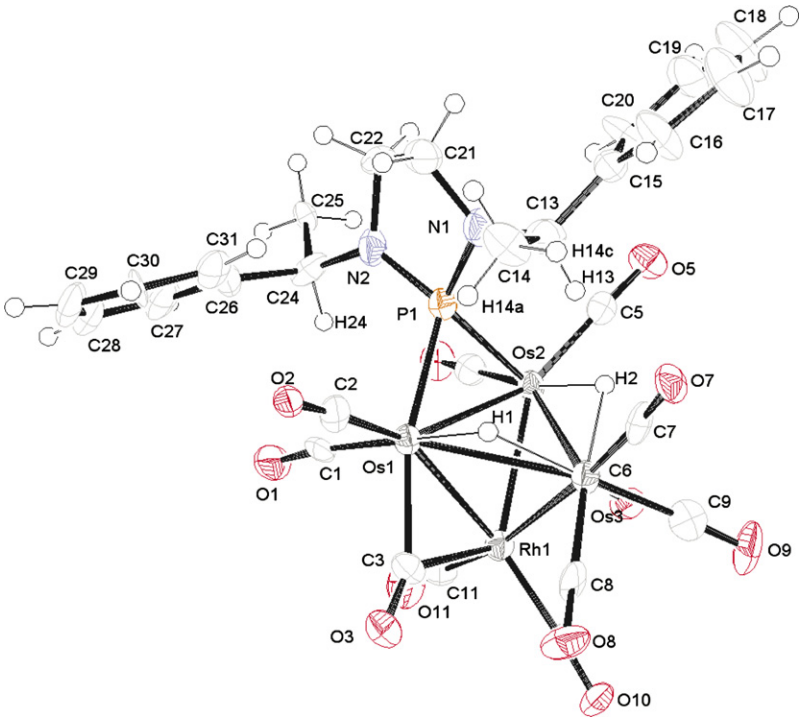

Fig. 3. ORTEP view of $H_2RhOs_3(CO)_{11}(\mu_2\text{-PNN})$ (**4**).

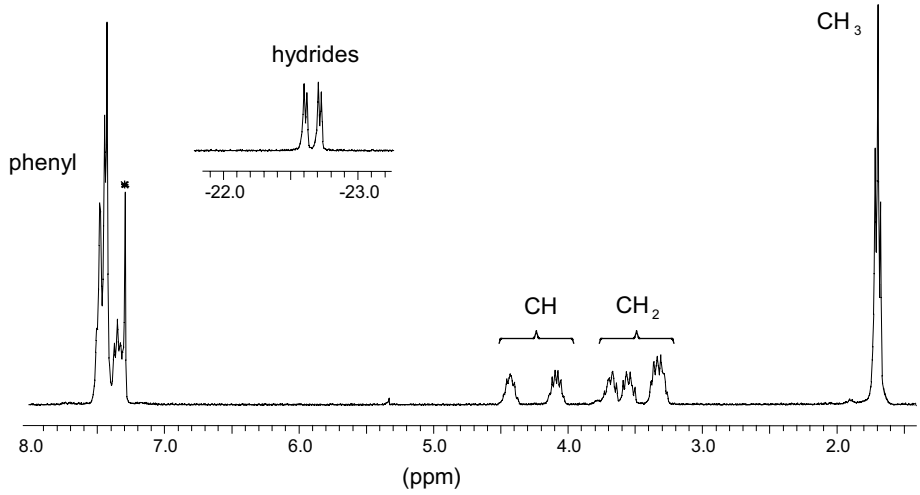

Fig. 4. ^{1}H NMR spectrum of $H_2RhOs_3(CO)_{11}(\mu_2\text{-PNN})$ (**4**), $CDCl_3$, 25 °C. Inset shows the hydride area of the spectrum. Residual signal of deuterochloroform is marked with an asterisk.

environment (see Fig. 3). This conformation of the molecular fragment contains a few very short nonbonding contacts between the hydrides and nearest protons of the ligand, H(13)–H(2) 2.19(2) Å, H(13)–H(1) 2.63(2) Å, H(14a)–H(1) 2.55(2) Å. These contacts are very probably determined by attractive electrostatic interaction between positively charged protons and negatively charged hydrides. The interaction of this sort (so-called ''dihydrogen bonding'') proved to be quite strong and in some cases may determine the particular configuration of the molecule as a whole [46–50]. The presence of these interactions in solution and conformational rigidity of (**4**) was confirmed by the ^{1}H NOE measurements, Fig. 5. The negative part of the NOE spectrum displays three crosspeaks between the hydride signals and resonances of the CH and CH_3 groups. These connectivities are related to through space interaction the hydrides with the chiral moiety disposed over the osmium triangle and allow easy assignment of the corresponding signals in the 1D spectrum through comparison of the NMR and X-ray data. The low frequency hydride resonance evidently corresponds to H(1) because of its short contacts with the protons of CH and CH_3

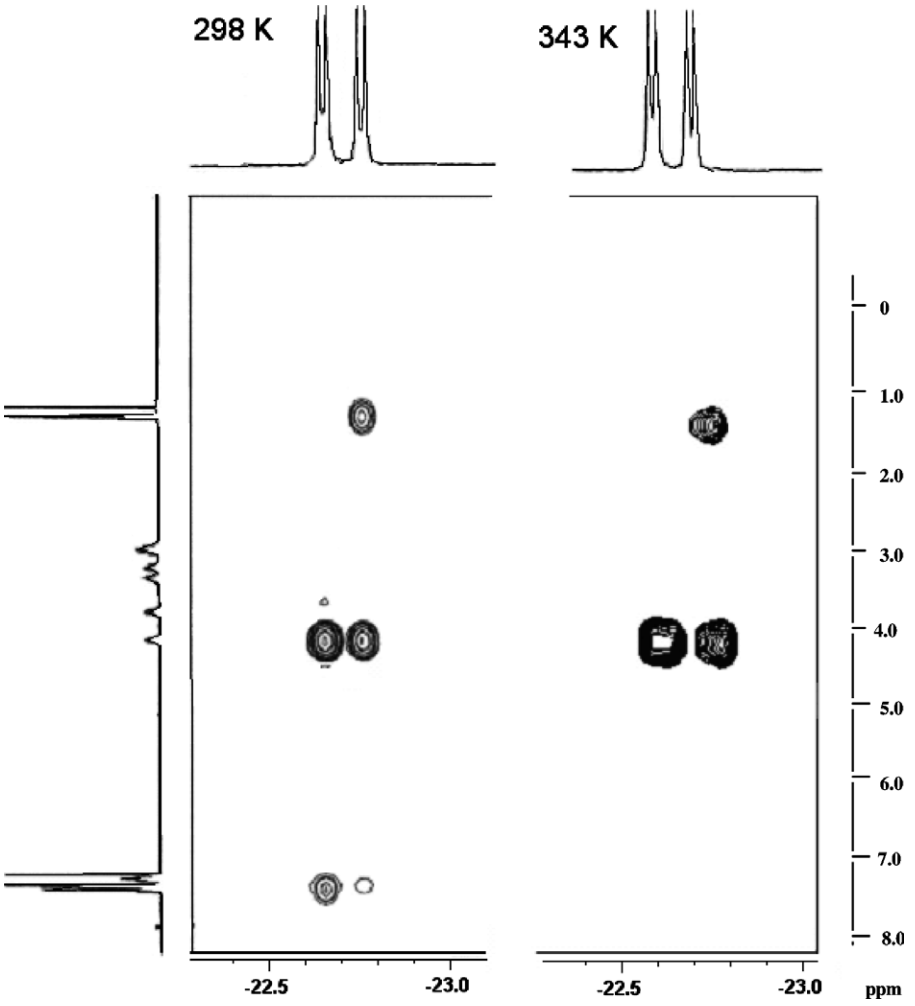

Fig. 5. Negative parts of the NOE spectrum of (**4**), C_6D_6, (a) 298 K and (b) 343 K.

groups, vide supra, which, in turn, are clearly displayed by the corresponding crosspeaks in the NOE spectrum. Thus, the high frequency hydride resonance is due to H(2), which has a short contact with the same CH proton. This interaction is visualized by another crosspeak related to the CH multiplet. A weaker NOE crosspeak connecting a resonance from the phenyl region and the high frequency hydride resonance has no direct support in the crystallographic data. It is, however, evident that rotation of the phenyl ring around the C(13)–C(15) bond may bring an *ortho* phenyl proton into the close vicinity of H(2) to give the conformation of the molecule which accounts for the NOE signal observed in the spectrum. This conformation proved to be a potential sink supported by ''dihydrogen bonding''. At higher temperature (+70 °C, Fig. 5b), this crosspeak disappears because of free rotation of the phenyl ring that results in averaging of rotational conformations to increase the average distance between correlated nuclei. Three other crosspeaks remain unchanged, even at this substantially higher temperature, which is indicative of the strength of the ''dihydrogen bonding'' in the molecule. This observation points once more to the importance of this type of interaction for the solution structure of hydride complexes containing hydrocarbon fragments in the ligand sphere.

4.3. $H_4Ru_4(CO)_{11}$-*R,R*-PHAZAN (**5**)

$H_4Ru_4(CO)_{12}$ reacts with *R,R*-PHAZAN in the presence of Me_3NO to give a monosubstituted cluster $H_4Ru_4(CO)_{11}$-*R,R*-PHAZAN in a reasonable yield. The solid state structure of this cluster was established by X-ray crystallography and an ORTEP view of the molecule is shown in Fig. 6; selected structural parameters are given in Table 2. The phosphine in (**5**) is coordinated through the phosphorus atom only and occupies a terminal position in the starting $H_4Ru_4(CO)_{12}$ cluster. Substitution of a CO ligand by the phosphine does not change the cluster electron count and the closed tetrahedral structure of the Ru_4-framework is unchanged. The configuration of the remaining 11 carbonyl ligands is nearly unchanged from the starting material. In contrast to the

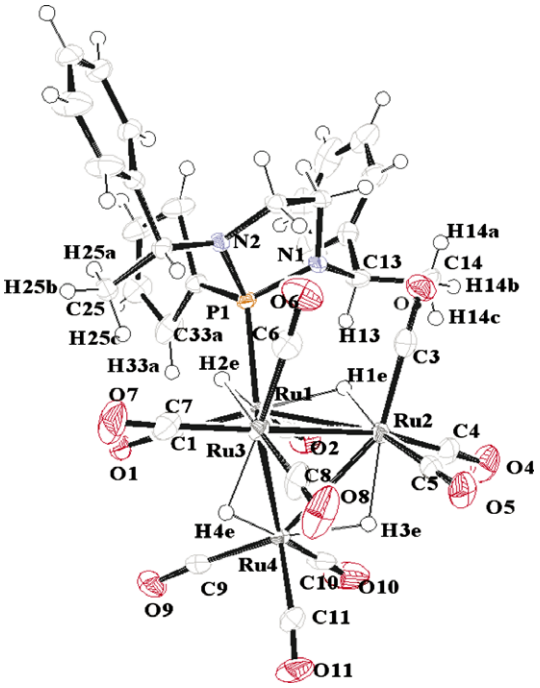

Fig. 6. ORTEP view of $H_4Ru_4(CO)_{11}(\kappa^1$-*R*,*R*-PHAZAN) (**5**).

$Rh_6(CO)_{16}$ derivative (**3**), the thienyl function of PHAZAN remains uncoordinated probably because of the mismatch of the short ligand bite angle and angular parameters of the terminal sites available at adjacent metal atoms. This situation is quite typical for bridging derivatives of $H_4Ru_4(CO)_{12}$. The only example of a bridging five-membered dimetallacycle in this system is $H_4Ru_4(CO)_{10}$(dppm) [51] with the Ru–Ru–P angles equal to ca. 92°, whereas unstrained configurations of the coordinating functions at the hydride bridged Ru–Ru bonds give the "Ru–Ru–X" angle values in the range 102–109° [52–55]. It has to be noted that a closely analogous P(thienyl)$_3$ ligand [56] also does not form a phosphino-thienyl bridge in the reaction with $H_4Ru_4(CO)_{12}$ to afford the monosubstituted $H_4Ru_4(CO)_{11}(\kappa^1$-P(thienyl)$_3$) cluster in a manner similar to (**5**). This observation shows that the bite angle of the phosphino-thienyl moiety (not the bulkiness of PHAZAN) is the main factor, which determines the coordination mode of these ligands.

In the solid state, $H_4Ru_4(CO)_{11}L$ mono-substituted derivatives containing phosphorus donor ligands display two motifs for the disposition of the hydrides over the "Ru_4" skeleton (**A** and **B** below).

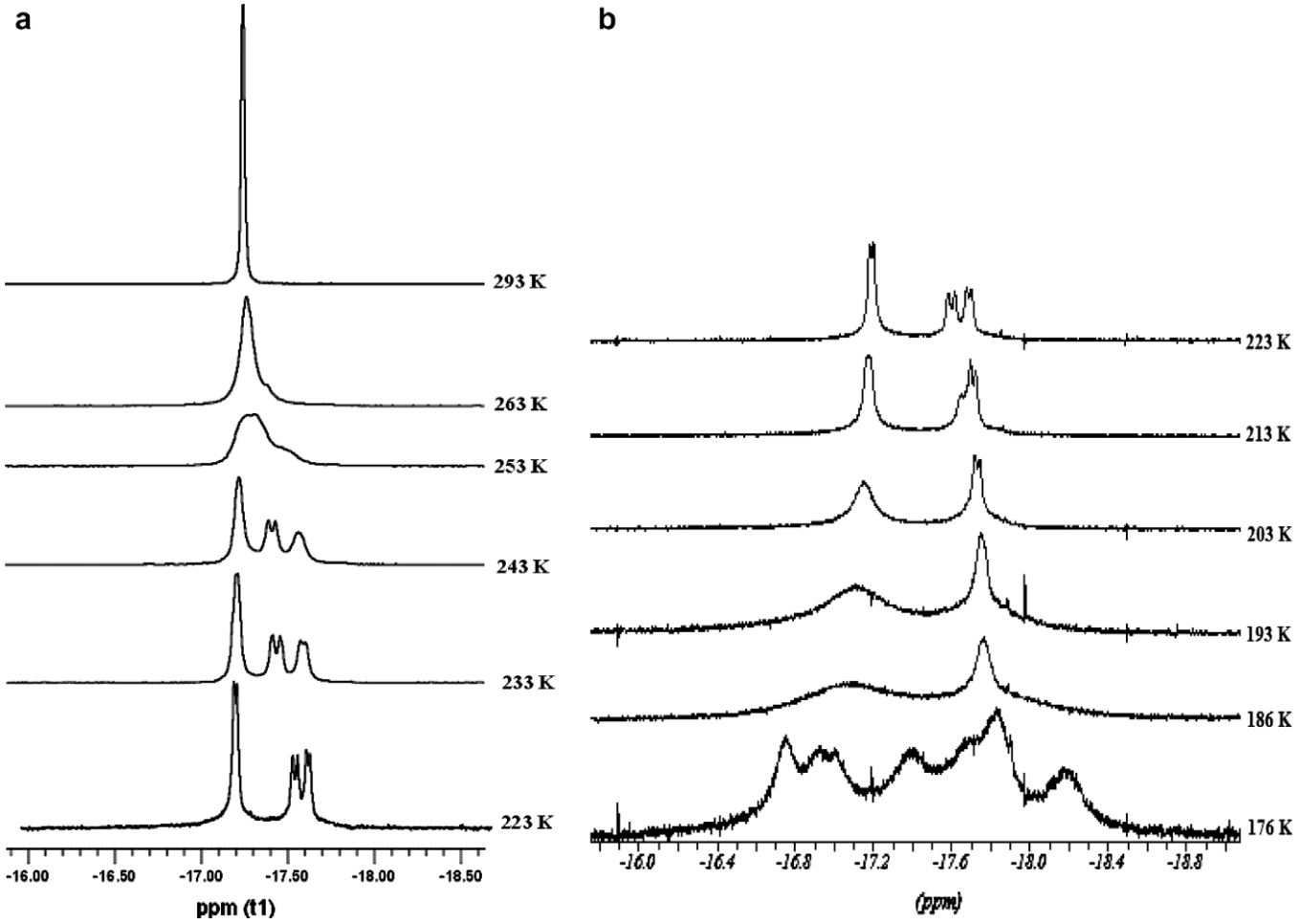

Fig. 7. VT ^{1}H NMR of (**5**) in the hydride region: (a) $CDCl_3$, (b) CD_2Cl_2.

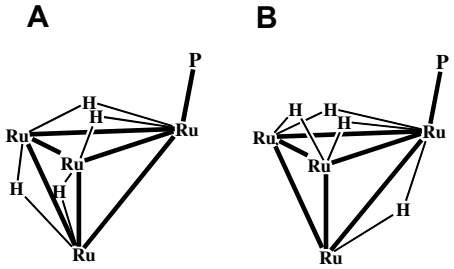

The isomer (**A**) was found in solid state structure of $H_4Ru_4(CO)_{11}(P(OMe)_3)$ [57], $H_4Ru_4(CO)_{11}(P(C_6F_5)_3)$ [57] and $H_4Ru_4(CO)_{11}(PPh_3)$ [58] whereas the $H_4Ru_4(CO)_{11}$-$(PPhMe_2)$ cluster [57] exists in form (**B**). Analysis of the difference Fourier map obtained for (**5**) indicates that the hydrides adopt the (**A**) structural pattern in the crystal cell of this complex. Completely in line with the general trend observed in the $H_4Ru_4(CO)_{12}$-substituted derivatives [56–58], the Ru–Ru edges spanned by the hydride ligands are the longest in the tetrahedron (see Table 2). This is also consistent with the structure of the "H_4Ru_4P" fragment corresponding to (**A**) isomer.

Similar to the other $H_4Ru_4(CO)_{11}(PR_3)$ derivatives studied by solution NMR spectroscopy [57,59], the hydride environment of (**5**) is fluxional at room temperature giving rise to a singlet at −17.29 ppm, which corresponds to fast exchange of all the hydrides at this temperature. The ^1H VT spectra of (**5**) are shown in Fig. 7. Lowering the temperature to 223 K results in the appearance three doublets (−17.21 ppm **2H**, 17.46 ppm **1H**, 17.59 ppm **1H**) with different P–H coupling constants: 4.9, 13.3 and 9.5 Hz, respectively. The phosphorus–hydride spin–spin interactions have been established by selective $^1H\{^{31}P\}$ decoupling experiments. The $^{31}P\{^1H\}$ NMR spectrum at 223 K displays one slightly broadened signal at 108.6 ppm, which at 176 K splits into two well resolved singlets at 105.7 and 111.6 ppm with relative intensities of ca. 3:1 (Fig. S8). In the same temperature range, the proton spectrum is complicated because of the dynamics of the hydrides, which are not static, even at 176 K. These observations can be explained by the exchange between the two isomeric forms of the hydride environment, for example between the (**A**) and (**B**) isomers shown above. This would be analogous to the dynamics found in the H_4Ru_4-$(CO)_{11}(PR_3)$ clusters, suggested earlier [57,59]. Under the framework of this hypothesis, the proton spectrum of the system at 223 K is a weighted average of the spectra of the exchange components. If the equilibrium mixture is enriched with one of them, the experimental spectrum is weighted with the dominating form. These characteristics fit well with the structure of the (**A**) isomer. For example, two high field doublets may be assigned to the hydrides adjacent to the phosphorus ligand, the values of the ^2J(P–H) coupling constants (9.5 and 13.3 Hz) being in a very good agreement with the other examples of *cis*-(P–H) interaction in the clusters of this sort [50]. The inequivalence of the symmetrically disposed hydrides is clearly due to the asymmetry of the phosphine ligand that makes these hydrides diastereotopic, which differentiates substantially their chemical shifts and coupling constants. The remote location of two other hydrides in the structure (**A**) leads to a substantially lower coupling constant, 4.9 Hz. Unfortunately, the minor form of the cluster cannot be characterized with the same level of certainty because, even at the lowest temperature (176 K) it was impossible to obtain the necessary resolution to assign the signals and to deduce the possible structure of the other isomer.

5. Conclusion

The optically active ligand *R*,*R*-PHAZAN (1,3-*bis*-[(1*R*)-1-Phenylethyl]-2-(2-thienyl)-1,3,2-diazaphospholane) reacts with various transition metal carbonyl clusters to give products which contain PHAZAN as either a bidentate ligand (with coordination through P and S) or a monodentate ligand (through P coordination); in addition, cleavage of the thienyl group can occur to give phosphido clusters. Edge-bridging coordination of PHAZAN in $Rh_6(CO)_{14}(\mu_2,\kappa^2$-*R*,*R*-PHAZAN) results in the formation of an additional two novel chiral centres and this bodes well for their future use in asymmetric catalysis. A variety of multinuclear NMR methods show that the solid state structures are retained in solution. In particular, it has been found that "dihydrogen bonding" between protons of organic ligand and hydrides plays an important role in retaining the conformation of the cluster molecules in solution.

Acknowledgments

Financial support from the Royal Society for an International Joint Awards grant and Journals Grants for International Authors (S.T) is gratefully acknowledged. M.T. appreciates greatly financial support from the University of Joensuu in a bilateral exchange program with St. Petersburg State University. The financial support of the Russian Foundation for Basic Research (Grant 05-03-33266) and of EPSRC (Grant EP/C0005643) is also gratefully acknowledged.

Appendix A. Supplementary material

CCDC 620564, 620565 and 620566 contain the supplementary crystallographic data for **3**, **4** and **5**. These data can be obtained free of charge via http://www.ccdc.cam.ac.uk/conts/retrieving.html, or from the Cambridge Crystallographic Data Centre, 12 Union Road, Cambridge CB2 1EZ, UK; fax: (+44) 1223-336-033; or e-mail: deposit@ccdc.cam.ac.uk. Supplementary data associated with this article (Figs. S1–S8) can be found, in the online version, at doi:10.1016/j.jorganchem.2007.03.008.

References

[1] G. Pracejus, H. Pracejus, Tetrahedron Lett. 18 (1977) 3497.
[2] A. Alexakis, S. Mutti, P. Mangeney, J. Org. Chem. 57 (1992) 1224.
[3] F. Slowinski, C. Aubert, M. Malacria, Tetrahedron Lett. 40 (1999) 5849.
[4] Z. Yang, Z. Zhou, K. He, L. Wang, G. Zhao, Q. Zhou, C. Tang, Tetrahedron: Asymmetry 14 (2003) 3937.
[5] B. Burns, N.P. King, H. Tye, J.R. Studley, M. Gamble, M. Wills, J. Chem. Soc., Perkin Trans. 1 (1998) 1027.
[6] B. Breit, J. Mol. Catal. A 143 (1999) 143.
[7] Z.-H. Yang, Z.-H. Zhou, L.-X. Wang, K.-Y. Li, Q.-L. Zhou, C.-C. Tang, Synth. Commun. 32 (2002) 2751.
[8] K. Li, Z. Zhou, G. Zhao, C. Tang, Heteroatom Chem. 14 (2003) 546.
[9] Y. Miyake, H. Takada, K. Ohe, S. Uemura, J. Chem. Soc., Perkin 1 (2000) 1595.
[10] G.E. Moreno, L. Quintero, S. Bernes, C. Anaya de Parrodi, Tetrahedron Lett. 45 (2004) 4245.
[11] F. Slowinski, C. Aubert, M. Malacria, J. Org. Chem. 68 (2003) 378.
[12] R. Hulst, N. Koen de Vries, B.L. Feringa, Tetrahedron: Asymmetry 5 (1994) 699.
[13] P.G. Devitt, T.P. Kee, Tetrahedron 51 (1995) 10987.
[14] P.G. Devitt, M.C. Mitchell, J.M. Weetman, R.J. Taylor, T.P. Kee, Tetrahedron: Asymmetry 6 (1995) 2039.
[15] S.R. Davies, M.C. Mitchell, C.P. Cain, P.G. Devitt, R.J. Taylor, T.P. Kee, J. Organomet. Chem. 550 (1998) 29.
[16] M. Bentov, L. David, E.D. Bergmann, J. Chem. Soc. (1964) 4750.
[17] S.P. Tunik, A.V. Vlasov, V.V. Krivykh, Inorg. Synth. 31 (1997) 239.
[18] S.A.R. Knox, J.W. Koepke, M.A. Andrews, H.D. Kaesz, J. Am. Chem. Soc. 97 (1975) 3942.
[19] P. Sundberg, B. Noren, B.F.G. Johnson, J. Lewis, P.R. Raithby, J. Organomet. Chem. 353 (1988) 383.
[20] B.T. Heaton, J.A. Iggo, I.S. Podkorytov, D.J. Smawfield, S.P. Tunik, R. Whyman, J. Chem. Soc., Dalton Trans. (1999) 1917.
[21] Z. Yang, Z. Zhou, K. He, L. Wang, G. Zhao, Q. Zhou, C. Tang, Tetrahedron: Asymmetry 14 (2003) 3937.
[22] Z. Otwinowski, W. Minor, in: C.W. CarterJr., R.M. Sweet (Eds.), Methods in Enzymology, Macromolecular Crystallography, part A, Academic Press, New York, USA, 1997, pp. 307–326.
[23] A. Altomare, M.C. Burla, M.C. Camalli, C. Giacovazzo, A. Guagliardi, A.G.G. Moliterni, G. Polidori, R. Spagna, J. Appl. Crystallogr. 32 (1999) 115.
[24] M.C. Burla, M.C. Camalli, B. Carrozzini, G.L. Cascarano, C. Giacovazzo, G. Polidori, R. Spagna, J. Appl. Crystallogr. 38 (2005) 381.
[25] G.M. Sheldrick, in: SHELXS97, Program for Crystal Structure Determination', University of Göttingen, Göttingen, Germany, 1997.
[26] L.J. Farrugia, J. Appl. Cryst 32 (1999) 837.
[27] G.M. Sheldrick, SHELXTL v. 6.14-1, Bruker Analytical X-ray Systems, Bruker AXS Inc., Madison, WI, USA, 2005.
[28] G.M. Sheldrick, SHELXL97, Program for Crystal Structure Refinement, University of Göttingen, Göttingen, Germany, 1997.
[29] M. Nardelli, J. Appl. Crystallogr. 32 (1999) 563.
[30] S.P. Tunik, I.O. Koshevoy, A.J. Poë, D.H. Farrar, E. Nordlander, M. Haukka, T.A. Pakkanen, Dalton Trans. (2003) 2457.
[31] E.V. Grachova, M. Haukka, B.T. Heaton, E. Nordlander, T.A. Pakkanen, I.S. Podkorytov, S.P. Tunik, Dalton Trans. (2003) 2468.
[32] D.V. Krupenya, S.I. Selivanov, S.P. Tunik, M. Haukka, T.A. Pakkanen, Dalton Trans. (2004) 2541.
[33] M. McPartlin, D.M.P. Mingos, Polyhedron 3 (1984) 1321.
[34] M.S. Owen, Polyhedron 7 (1988) 253.
[35] V.D. Patel, A.A. Cherkas, D. Nucciarone, N.J. Taylor, A.J. Carty, Organometallics 4 (1985) 1792.
[36] S.B. Colbran, P.T. Irele, B.F.G. Johnson, F.J. Lahoz, J. Lewis, P.R. Raithby, J. Chem. Soc., Dalton Trans. (1989) 2023.
[37] A.J. Deeming, S. Doherty, M.W. Day, K.I. Hardcastle, H. Minassian, J. Chem. Soc., Dalton Trans. (1991) 1273.
[38] H.G. Ang, C.H. Koh, L.L. Koh, W.L. Kwik, W.K. Leong, W.Y. Leong, J. Chem. Soc., Dalton Trans. (1993) 847.
[39] A.J. Deeming, M.B. Smith, J. Chem. Soc., Dalton Trans. (1993) 3383.
[40] W.R. Cullen, S.J. Rettig, T.C. Zheng, Organometallics 12 (1993) 688.
[41] A.J. Arce, A.J. Deeming, Y. De Sanctis, A.M. Garcia, J. Manzur, Organometallics 13 (1994) 3381.
[42] W.R. Cullen, S.J. Rettig, H. Zhang, Inorg. Chim. Acta 251 (1996) 53.
[43] B.F.G. Johnson, J. Lewis, E. Nordlander, P.R. Raithby, Inorg. Chim. Acta 259 (1997) 345.
[44] A.J. Arce, R. Machado, Y. De Sanctis, T. Gonzalez, R. Atencio, A.J. Deeming, Inorg. Chim. Acta 344 (2003) 123.
[45] V.I. Ponomarenko, T.S. Pilyugina, V.D. Khripun, E.V. Grachova, S.P. Tunik, M. Haukka, T.A. Pakkanen, J. Organomet. Chem. 691 (2006) 111.
[46] T.B. Richardson, T.F. Koetzle, R.H. Crabtree, Inorg. Chim. Acta 250 (1996) 69.
[47] W. Xu, A.J. Lough, R.H. Morris, Can. J. Chem. 75 (1997) 475.
[48] Y.A. Abramov, L. Brummer, W.T. Klooster, R.M. Bullock, Inorg. Chem. 37 (1998) 6317.
[49] R. Custelcean, J.E. Jackson, Chem. Rev. 101 (2001) 1963.
[50] S.P. Tunik, T.S. Pilyugina, I.O. Koshevoy, S.I. Selivanov, M. Haukka, T.A. Pakkanen, Organometallics 23 (2004) 568.
[51] F. Mansilla, G. Lavigne, J.J. Bonnet, Acta Crystallogr., Sect. C 42 (1986) 1011.
[52] R.D. Wilson, S.M. Wu, R.A. Love, R. Bau, Inorg. Chem. 17 (1978) 1271.
[53] M.A. Churchill, R.A. Lashewicz, J.R. Shapley, S.I. Richter, Inorg. Chem. 19 (1980) 1277.
[54] J. Puga, A. Arce, D. Braga, N. Centritto, F. Grepioni, R. Castillo, J. Ascanio, Inorg. Chem. 26 (1987) 867.
[55] P. Homanen, R. Persson, M. Haukka, T.A. Pakkanen, E. Nordlander, Organometallics 19 (2000) 5568.
[56] T.M. Rasanen, S. Jaaskelainen, T.A. Pakkanen, J. Organomet. Chem. 553 (1998) 453.
[57] M.G. Ballinas-Lopez, E.V. Garcia-Baez, M.J. Rosales-Hoz, Polyhedron 22 (2003) 3403.
[58] A.U. Haerkoenen, M. Ahlgren, T.A. Pakkanen, J. Pursiainen, J. Organomet. Chem. 530 (1997) 191.
[59] S. Aime, M. Botta, R. Gobetto, L. Milone, D. Osella, R. Gellert, E. Rosenberg, Organometallics 14 (1995) 3693.